Time-resolved photoluminescence measurements of InGaAs/InP multiple-quantum-well structures at 1.3-μm wavelengths by use of germanium single-photon avalanche photodiodes

G. S. Buller, S. J. Fancey, J. S. Massa, A. C. Walker, S. Cova, and A. Lacaita

A commercially available germanium avalanche photodiode operating in the single-photon-counting mode has been used to perform time-resolved photoluminescence measurements on InGaAs/InP multiple-quantum-well structures. Photoluminescence in the spectral region of 1.3–1.48 μm was detected with picosecond timing accuracy by use of the time-correlated single-photon counting technique. The carrier dynamics were monitored for excess photogenerated carrier densities in the range 10^{18}–10^{15} cm^{-3}. The recombination time is compared for similar InGaAs-based quantum-well structures grown by use of different epitaxial processes.

Key words: Time-resolved photoluminescence, InGaAs/InP, multiple quantum wells, germanium avalanche photodiodes.

1. Introduction

Time-resolved single-photon detection in the spectral region beyond 1 μm is of interest for a number of applications in the telecommunications industry and the biological sciences. Recent work[1–4] has reported the performance of commercially available Ge and InGaAs avalanche photodiodes (APD's) biased above breakdown in the so-called Geiger regime, where a single incoming photon can trigger an avalanche. In this paper, we report the application of single-photon counting germanium APD's to the measurement of time-resolved photoluminescence (TRPL), with picosecond temporal resolution, from semiconductor structures emitting in the 1.3–1.48-μm spectral region.

Silicon single-photon avalanche diodes (SPAD's) have demonstrated a timing accuracy of ~20 ps (Ref. 5) for small-diameter (~8-μm) devices. However, these devices can only operate with high efficiency (i.e., greater than a few percent) at wavelengths less than ~1.1 μm. Single-photon detection is possible up to ~1.2 μm with photomultiplier tubes that use a cooled S-1 photocathode. However, at this wavelength their quantum efficiency is $<10^{-4}$ and falls rapidly with increasing wavelength. Single-photon detectors based on cooled germanium avalanche devices offer the possibility of high-speed, high-sensitivity, single-photon detection at wavelengths up to ~1.5 μm.

TRPL has been used extensively to study the excess carrier dynamics in structures based on the direct-gap semiconductors GaAs and ZnSe.[6,7] The excess carrier decay in such structures is of considerable importance in the design and fabrication of optoelectronic devices such as LED's, laser diodes, and modulators, in which the carrier lifetime can determine the device performance. In the past, a number of techniques have been used to study carrier recombination in semiconducting materials with an absorption edge at wavelengths greater than 1.1 μm. Examples include nonlinear pump-probe techniques,[8,9] nonlinear photoluminescence (PL) autocorrelation,[10] nonlinear frequency-dependent transmission,[11] luminescence upconversion,[12] and analog TRPL.[13] The first three techniques require photogenerated carrier densities of $>10^{17}$ cm^{-3} and, because of their small dynamic range, provide only a limited description of the carrier decay kinetics.

G. S. Buller, S. J. Fancey, J. S. Massa, and A. C. Walker are with the Department of Physics, Heriot-Watt University, Riccarton, Edinburgh EH14 4AS, UK. S. Cova and A. Lacaita are with the Dipartimento di Elettronica e Informazione, Politecnico di Milano, Piazza L. da Vinci 32, 20133 Milano, Italy.

Received 22 March 1995; revised manuscript received 13 July 1995.
0003-6935/96/060916-06$06.00/0

Luminescence upconversion provides better sensitivity but requires a much more complex optical setup. The main advantage offered by such techniques is that they are based on optical pulse correlation, and thus the temporal resolution is limited only by the excitation pulse duration. However, the required use of an optical delay can make the measurement of long decay times difficult. Photon-counting detectors, when used with the time-correlated single-photon counting technique, permit the monitoring of PL decays over large dynamic ranges in signal intensity (e.g., $>10^4$). In addition, these detectors are compatible with a wide range of decay times (e.g., tens of picoseconds to microseconds) and can offer a much higher detection sensitivity than the techniques mentioned above.

The instrument used in this study[14] (based on an Edinburgh Instruments LifeMap) is constructed around a standard infinite-conjugate microscope, shown in Fig. 1. The laser excitation, optical trigger signal, and resulting PL are routed to and from the sample by use of polarization optics located within the microscope column. A number of passively Q-switched picosecond laser diodes, developed at the Ioffe Physico-Technical Institute, St. Petersburg, Russia,[15] are available as excitation sources. Previously, a similar optical system based on a silicon SPAD has been used to study carrier dynamics in various III–V (Ref. 16) and II–VI (Ref. 17) materials, in which the required detection wavelength was <1 μm. The use of high-numerical-aperture optical components ensures a high PL-collection efficiency and, combined with a small-area detector (a 30-μm-diameter Ge SPAD was used in these experiments), results in a ~5-μm-diameter region in the sample plane being imaged onto the detector. In this optical system, changes to the microscope objective and detector focusing lenses permit optimization of spatial resolution and PL-collection efficiency to suit particular sample measurements.

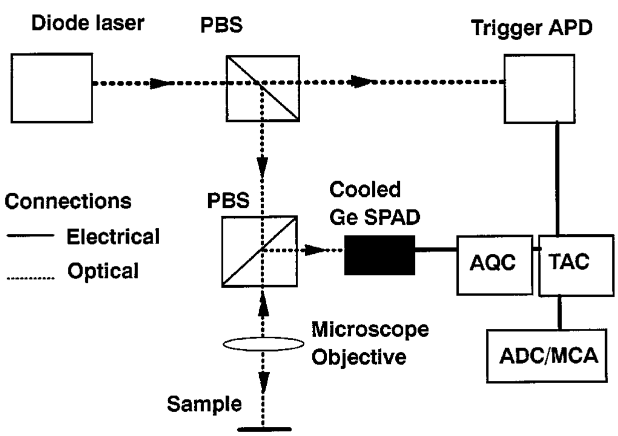

Fig. 1. Schematic diagram of the TRPL setup, showing the polarizing beam splitters (PBS's). The excitation pulses are directed toward the sample by the upper PBS. A small fraction of the pulse energy is transmitted through this PBS to provide a signal for the analog APD, which triggers the time-to-amplitude converter (TAC). The excited luminescence is collected by the microscope objective and reflected toward the cooled Ge SPAD by the lower PBS. The active quenching circuit (AQC) detects the avalanche from a photon event, quenches this avalanche, and emits a timing pulse. The time separation of the timing pulse and the trigger pulse is measured by the TAC, which outputs an analog voltage signal to the analog-to-digital converter (ADC). The digital output is stored in the multichannel analyzer (MCA) and displayed as a histogram.

The detector used for the TRPL measurements presented in this paper was a commercially available germanium APD (Fujitsu FPD13R31KS with the fiber-pigtail packaging removed) designed for operation in the analog mode. It was cooled in a liquid nitrogen Dewar to 77 K, to reduce the dark-count rate (i.e., the rate of avalanches triggered by thermally generated carriers).[18]

The Geiger-mode APD was actively quenched with a commercially available active-quenching circuit[19] (Silena Model 8619). A schematic of the timing system is also shown in Fig. 1. On detection of an avalanche current pulse, the active-quenching circuit lowers the diode bias voltage below the breakdown value, thus quenching the avalanche process. Simultaneously, the circuit sends a timing signal to the time-to-amplitude converter (TAC), which starts the timing process. A fraction of the pump-laser pulse is detected by a fast-analog APD (Optoelectronics Model PAD230), which after an appropriate delay is used to stop the TAC. The TAC is operated in this reverse mode[20] to ensure that the timing sequence is only initiated on detection of an avalanche event, rather than on every laser pulse. The output from the TAC is in the form of an analog voltage pulse, with an amplitude that is proportional to the timing difference between arrival of the avalanche signal and the delayed laser pulse. This timing signal is digitized by the analog-to-digital converter and then stored in the multichannel analyzer, which contains 4096 timing channels. Over many laser pulses, the multichannel analyzer accumulates data in the form of a histogram of number of counts versus time. If the count rate is sufficiently low to ensure that the probability of more than one photon arriving at the detector during each excitation cycle is low, then the histogram will be an accurate representation of the photon-emission probability distribution, i.e., in this case the PL decay.[21] At high photon-detection rates, when this condition is not met, the resulting probability distribution will be skewed toward the initial part of the timing sequence, because only the first photon to be detected is counted in any excitation cycle, and the subsequent photon events occurring in that timing window cannot be detected because of the relatively long system dead time (typically >1 μs). The result of this condition is that the histogram is not a true representation of the PL decay. Techniques have been developed to compensate for this problem and one approach, that of Coates,[22] is described in Section 2.

In order to reduce the dark-count rate, the detector was operated in a gated mode, as used previously by

Lacaita *et al.*[3] In this case, the bias was held above V_B for a 200-ns period, in synchronization with the excitation pulse. Reducing the net flow of charge through the device by gating lowers the dark-count rate, as it reduces the trap occupancy in the avalanche region, and hence the thermal carrier excitation rate. In addition, the excitation repetition rate was kept low, typically 1–10 kHz, to ensure the emptying of traps by thermal emission before the next cycle began. A thermal-emission time of ~200 µs has been reported in germanium at this temperature,[3] and this is consistent with our measurements. The dark-count rate for a 200-ns gate at a repetition rate of 10 kHz was ~250 Hz for a bias of 0.6 V above breakdown. At this bias, the quantum efficiency of the APD at 1.3 µm was measured to be ~10%, consistent with that reported by Lacaita *et al.*[3]

To assess the temporal response of the system, a passively *Q*-switched InGaAs/InP laser diode was used as the excitation source. The pulse length was ~15 ps full width at half-maximum (FWHM) at a wavelength of 1.3 µm. Figure 2 shows the recorded instrumental response with the Ge APD biased 0.6 V above breakdown ($V_B = 22.5$ V) and cooled to 77 K. This response had a FWHM of ~310 ps. Increasing the bias level reduces the width of the temporal profile; for example, at 2 V above V_B a FWHM of ~130 ps was obtained, but at the expense of a much higher dark-count rate, in this case reducing the signal-to-background ratio by approximately a factor of 3.

2. Experimental Results

With the system described above, TRPL measurements were performed on three similar $In_{0.53}Ga_{0.47}As$/InP multiple-quantum-well (MQW) structures grown by use of different techniques. Sample 1 comprised 65.5 periods of 30-Å $In_{0.53}Ga_{0.47}As$ wells with 50-Å InP barriers and was grown by use of solid-source molecular beam epitaxy at the Engineering and Physical Science Research Council III–V Semiconductor Facility, Sheffield, UK. Sample 2 had an identical structure but was grown by use of chemical beam epitaxy at Centro Studi e Laboratori Telecomunicazioni S.p.A, Torino, Italy. The room-temperature PL-emission peaks from these samples were at 1.31 µm. Sample 3 comprised 40.5 periods of 50-Å $In_{0.53}Ga_{0.47}As$ wells with 50-Å InP barriers and was grown by use of gas-source molecular beam epitaxy at BT Laboratories, Ipswich, UK. The room-temperature PL-emission peak from this latter structure was at the longer wavelength of 1.48 µm.

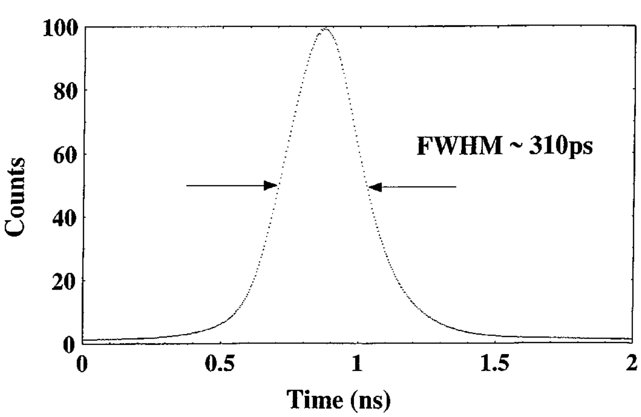

Fig. 2. Typical instrumental response (FWHM ~ 310 ps) obtained with a 10-ps-duration laser input pulse at a wavelength of 1.3 µm. The SPAD was biased at 0.6 V above V_B.

In the TRPL measurements presented below, the detection rate was typically >60% of the laser repetition rate in order to maximize the detected PL signal relative to the background. As mentioned above, it is usual in time-correlated single-photon counting experiments to maintain a low count rate compared with the excitation repetition rate to avoid pulse pileup effects. If the detection rate is kept to <5% of the laser rate, then pileup effects can usually be regarded as insignificant.[21] Hence, for these examples, it was necessary to use the pileup-correction method described by Coates[22] to extract a true representation of the PL decays from the available raw data. A source of experimental error was radio-frequency (RF) pickup from the pulsed high-current source used for driving the laser diode. Because of the particular frequency of the RF emission, this problem was only evident in the case of the longest decay, that from sample 1. To reduce this problem, the raw PL data were divided by the results of a background measurement taken with no light signal present. These two correction processes are illustrated in Fig. 3. Both of these correction procedures imply some increase in noise. In fact, the correction factors, computed from the experimental data, are affected by random fluctuations, which are combined with the Poisson fluctuations of the raw data. It is expected that the latter effect can be greatly reduced by use of improved detector packaging and electromagnetic shielding.

The PL decays at the peak emission wavelength for the three samples under study are shown in Fig. 4. In each case, the excitation source was a passively *Q*-switched picosecond GaAs/AlGaAs laser diode emitting at a wavelength of 859 nm. The laser pulse energy was ~3 pJ, with a pulse duration of ~10 ps (FWHM). This output was focused to a ~2-µm-diameter spot on the sample surface, yielding a peak photogenerated carrier density of ~10^{18} cm^{-3}. The detector bias was 23.1 V (0.6 V above V_B). The PL signals were discriminated from the excitation source with a combination of appropriate edge and bandpass filters.

It can be seen that the PL signals decay on significantly different time scales, and this would seem to indicate a considerable difference in the material quality of these three samples. The dominant exponential time constants for these decays, obtained by use of reconvolution analysis with the measured instrumental response, were 240 ps, 5 ns, and 28 ns for samples 3, 2, and 1, respectively. The temporal breadth of these measurements indicates

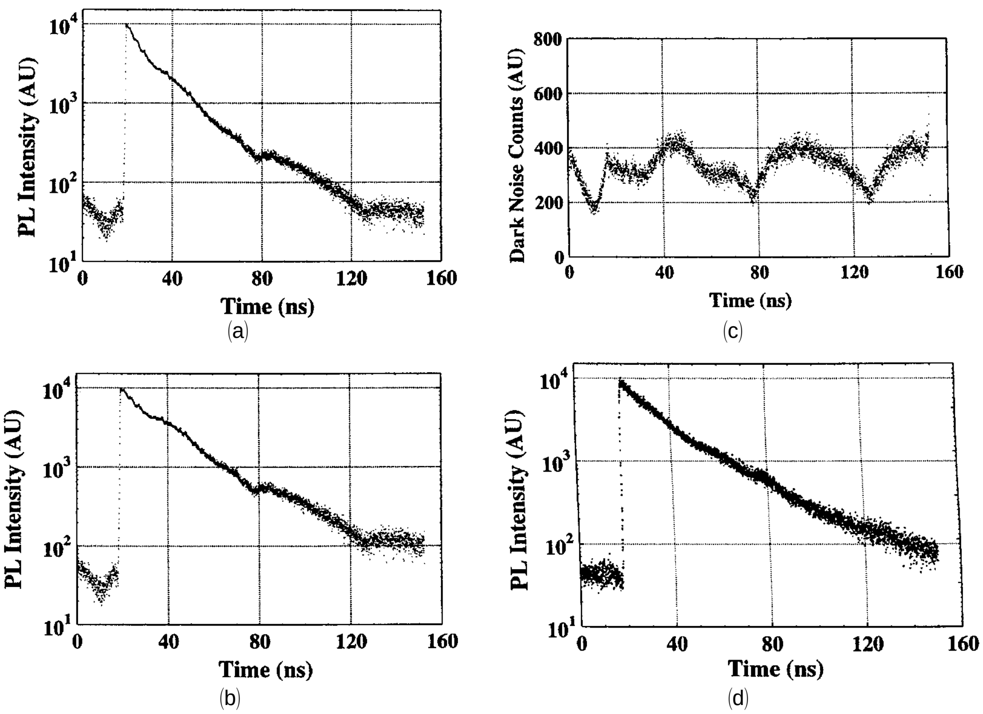

Fig. 3. Processes involved in data correction are illustrated as follows, using data from sample 1. It should be noted that the correction for RF interference was not required for either of the other two samples. (a) Raw data recorded at 64% of the laser repetition rate. RF pickup is evident. (b) Data after correction for pulse pileup. (c) Background counts recorded with no light reaching the detector (note the linear scale). (d) Time-resolved PL signal from sample 1 after division by background.

both the versatility and the necessity of this technique for studying the carrier dynamics in real semiconductor structures. With a typical instrumental response of <0.5 ns (FWHM), it is possible that decays as short as ~50 ps may be resolved with

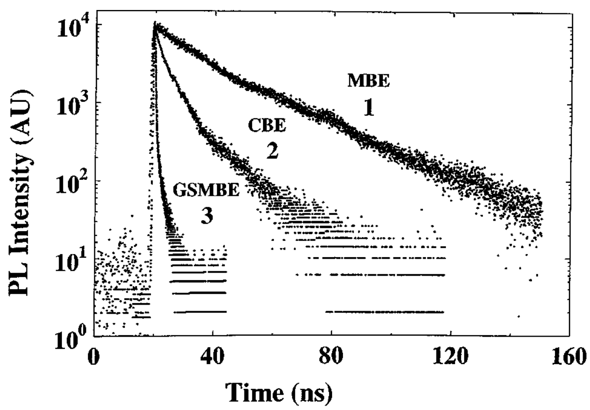

Fig. 4. TRPL measurements on sample 1 [molecular beam epitaxy (MBE) grown], sample 2 [chemical beam epitaxy (CBE) grown] and sample 3 [gas-source molecular beam epitaxy (GSMBE) grown] with a ~2-μm excitation spot size. The detection wavelengths were 1.3 μm (samples 1 and 2) and 1.48 μm (sample 3). The PL was discriminated from the pump with a filter centred on 1.3 μm with a 25-nm bandpass (samples 1 and 2) and a silicon edge filter transmitting above ~1.0 μm (sample 3). The excitation energy was 3 pJ/pulse, at a wavelength of 859 nm. This initial photogenerated carrier density was $\sim 10^{18}$ cm^{-3}. The decays shown are after correction for pulse pileup. The results for sample 1 have also been corrected for background RF interference, as described in the text.

reconvolution analysis. This commonly used approach involves iteratively convolving the instrumental response with a candidate theoretical model (e.g., exponential decay) until the best fit to the data is obtained with respect to a number of variable parameters (see chapter 2 of Ref. 21 and references therein).

Pickin and David[23] proposed that the principal route for carrier recombination in III–V quantum-well structures is through nonradiative centers associated with the well–barrier interfaces. Because there is greater coupling between the carrier wave functions and the interface states in these quantum-confined structures than in bulk material, the recombination rate will be significantly higher. It will also be linear with carrier density—resulting in an exponential PL decay—if the occupancy of the surface states is in either of the Shockley–Read low-level or high-level regimes[24] for the duration of the decay. In the low-level regime, the interface recombination centers never become saturated, meaning that the decay rate of the interband transition associated with the PL emission will depend on the carrier trapping rate. In the high-level regime, the traps will be saturated quickly and the PL decay will depend mainly on the rate at which the traps empty.

Clearly, the PL decays in Fig. 4 do not exhibit the single exponential form characteristic of a linear recombination process. One reason for this is that in using a small excitation spot, carriers can diffuse transversely out of the region of the sample viewed by the detector. Under these circumstances, the PL decay will have a nonlinear diffusive component in

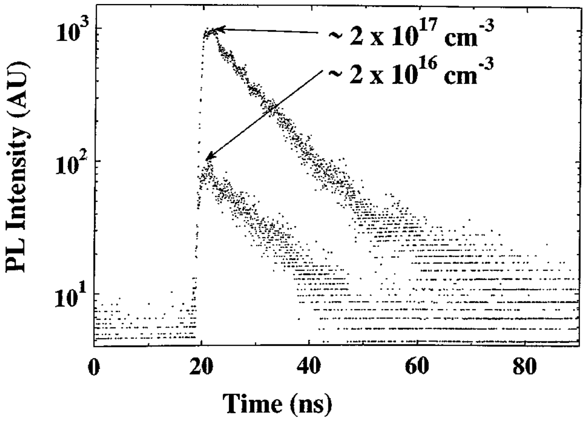

Fig. 5. Two TRPL decays from sample 2 measured at 1.288 to 1.312 μm with a large (15-μm-diameter) excitation spot size and different excitation pulse energies. The initial photogenerated carrier densities are as indicated. The PL is found to decay exponentially in the absence of diffusion, and the two curves indicate that the limit of detection at 1.3 μm is $\sim 10^{15}$ excited carriers cm^{-3} when the optical system described in the text is used.

addition to the linear interface recombination term. When the size of the excitation spot on the sample surface is increased, thus minimizing the transverse carrier concentration gradient across the small-sample-detection region, the effects of transverse diffusion on the TRPL measurements can be considerably reduced, as shown in Fig. 5.

In this case, the spot size was increased to ~ 15 μm diameter, and TRPL measurements were made, from sample 2, at several different initial photogenerated carrier densities. In each case, the decays assume a predominantly single exponential form, in contrast to the nonexponential decays shown in Fig. 4. The observation of single exponential decays is consistent with previous TRPL measurements on GaAs/AlGaAs multiple quantum wells.[25] Decays from two different initial excitation densities are shown in Fig. 5, and these indicate that the lowest carrier density at which the PL can be discriminated from the background is $\sim 10^{15}$ cm^{-3}. The PL decay-time constant for this sample was approximately 10 ns. This is consistent with the time constant measured at the later part of the decay shown in Fig. 4, where the initial part of the decay was dominated by carrier outdiffusion.

3. Conclusion

Subnanosecond TRPL measurements have been successfully performed on InGaAs/InP MQW structures at emission wavelengths of 1.3 and 1.48 μm with a cooled, commercially available germanium APD operated in the photon-counting mode. The carrier dynamics in these MQW structures have been studied at photogenerated carrier densities in the range 10^{18}–10^{15} cm^{-3}. The absolute temporal resolution of the TRPL system is estimated to be ~ 50 ps when reconvolution analysis is used. The PL decays indicate that the dominant recombination process in these structures is linear with carrier density and that there are large differences in the decay time scales of near-identical samples grown with different processes.

Future research will concentrate on two main areas: (a) better understanding of the InGaAs MQW material with more detailed investigation of the effects of different growth and processing techniques and (b) provision of better SPAD's suitable for this wavelength range. The latter investigation will include a study of InGaAs SPAD's that will operate at longer wavelengths, including the strategically important 1.55-μm-wavelength region. The use of smaller-area devices with a lower dark count should enhance the sensitivity of the direction system and provide an unproved temporal response.

The Heriot-Watt University group acknowledges the financial support of the Royal Society Paul Instrument Fund and the UK Engineering and Physical Science Research Council (EPSRC). This work was partly supported by North Atlantic Treaty Organization Cooperative Research Grant No. 920218. SJF is supported by an EPSRC Cooperative Award in Science and Engineering in conjunction with Edinburgh Instruments, Ltd. The authors would like to thank David Neilson for many helpful discussions and BT Laboratories, UK, for the provision of sample 3.

References

1. A. Lacaita, S. Cova, F. Zappa, and P. A. Francese, "Subnanosecond single-photon timing with commercially available germanium photodiodes," Opt. Lett. **18,** 75–77 (1993).
2. F. Zappa, A. Lacaita, S. Cova, and P. Webb, "Nanosecond single-photon timing with InGaAs/InP photodiodes," Opt. Lett. **19,** 846–848 (1994).
3. A. Lacaita, P. A. Francese, F. Zappa, and S. Cova, "Single-photon detection beyond 1 μm: performance of commercially available germanium photodiodes," Appl. Opt. **33,** 6902–6918 (1994).
4. P. C. M. Owens, J. G. Rarity, P. R. Tapster, D. Knight, and P. D. Townsend, "Photon counting with passively quenched germanium avalanche photodiodes," Appl. Opt. **33,** 6895–6901 (1994).
5. S. Cova, A. Lacaita, M. Ghioni, G. Ripamonti, and T. A. Louis, "20 ps timing resolution with single photon avalanche diodes," Rev. Sci. Instrum. **60,** 1104–1110 (1989).
6. R. J. Nelson and R. G. Sobers, "Minority-carrier lifetime and internal quantum efficiency of surface-free GaAs," Appl. Phys. Lett. **49,** 6103–6107 (1978).
7. J. E. Potts, H. Cheng, S. H. Park, B. Fluegel, M. Joffre, S. W. Koch, and N. Peyghambrian, "Excitonic optical nonlinearities in ZnSe epitaxial films," in *Optical Computing and Nonlinear Materials,* N. Peyghambarian, ed., Proc. Soc. Photo-Opt. Instrum. Eng. **881,** 107–113 (1988).
8. J. E. Ehrlich, D. T. Neilson, A. C. Walker, G. T. Kennedy, R. S. Grant, W. Sibbett, and M. Hopkinson, "Carrier lifetimes in MBE and MOCVD InGaAs quantum wells," Semiconduct. Sci. Technol. **8,** 307–309 (1993).
9. M. E. Prise, M. R. Taghizadeh, S. D. Smith, and B. S. Wherrett, "Picosecond measurement of Auger recombination rates in InGaAs," Appl. Phys. Lett. **45,** 652–654 (1984).
10. I. Brener, D. Gershoni, D. Ritter, M. B. Panish, and R. A. Hamm, "Decay times of excitons in lattice-matched

InGaAs/InP single quantum wells," Appl. Phys. Lett. **58,** 965–967 (1991).

11. D. A. H. Mace and M. J. Adams, "Carrier recombination time measurements in InAlAs/InGaAs multiple quantum wells using non-linear frequency dependent transmission," Semicond. Sci. Technol. **5,** 105–107 (1990).
12. R. Kersting, X. Q. Zhou, K. Wolter, D. Grutzmacher, and H. Kurz, "Subpicosecond luminescence study of carrier transfer in InGaAs/InP multiple quantum wells," Superlattices Microstructures **7,** 345–348 (1990).
13. B. Sermage, J. P. Heritage, and N. K. Dutta, "Temperature dependence of carrier lifetime and Auger recombination in 1.3-µm InGaAsP," J. Appl. Phys. **57,** 5443–5449 (1985).
14. T. A. Louis, G. Ripamonti, and A. Lacaita, "Photoluminescence lifetime microscope spectrometer based on time-correlated single-photon counting with an avalanche diode detector," Rev. Sci. Instrum. **61,** 11–22 (1990).
15. Z. I. Alferov, A. B. Zuravlev, E. L. Portnoi, and N. M. Stel'makh, "Picosecond pulses from Q-switched injection heterostructure lasers," Sov. Tech. Phys. Lett. **12,** 452–453 (1986).
16. J. S. Massa, G. S. Buller, A. C. Walker, J. L. Oudar, E. V. K. Rao, B. G. Sfez, and R. Kuselewicz, "Evidence of carrier confinement in nonlinear GaAs/AlGaAs multiple quantum-well microresonators fabricated using alloy mixing techniques," Appl. Phys. Lett. **61,** 2205–2207 (1992).
17. G. S. Buller, J. S. Massa, and A. C. Walker, "All-solid-state microscope-based system for picosecond time-resolved photoluminescence measurements on II–VI semiconductors," Rev. Sci. Instrum. **63,** 2994–2998 (1992).
18. R. H. Haitz, "Mechanisms contributing to the noise pulse rate of avalanche diodes," J. Appl. Phys. **36,** 3123–3131 (1965).
19. S. Cova, A. Longoni, and A. Andreoni, "Towards picosecond resolution with single-photon avalanche diodes," Rev. Sci. Instrum. **52,** 408–412 (1981).
20. B. T. Turko, J. A. Nairn, and K. Sauer, "Single photon timing system for picosecond fluorescence lifetime measurements," Rev. Sci. Instrum. **54,** 118–120 (1983).
21. D. V. O'Connor and D. Phillips, *Time-Correlated Single Photon Counting* (Academic, New York, 1983).
22. P. B. Coates, "The correction for photon 'pile-up' in the measurement of radiative lifetimes," J. Phys. E **1,** 878–879 (1968).
23. W. Pickin and J. P. R. David, "Carrier decay in GaAs quantum wells," Appl. Phys. Lett. **56,** 268–270 (1990).
24. W. Shockley and W. T. Read Jr., "Statistics of recombinations of holes and electrons," Phys. Rev. **87,** 835–842 (1952).
25. J. E. Fouquet and A. E. Siegman, "Room-temperature photoluminescence times in GaAs/$Al_xGa_{1-x}As$ structure," Appl. Phys. Lett. **46,** 280–282 (1985).